Power Density Spectra of Gamma-Ray Bursts

Andrei M. Beloborodov, Boris E. Stern, and Roland Svensson

Stockholm Observatory, Saltsjöbaden SE-133 36, Sweden

Abstract. The longest gamma-ray bursts (GRBs) display power-law power density spectra (PDSs). Shorter bursts have PDSs more strongly affected by statistical fluctuations. The underlying power law can then be reproduced with high accuracy by averaging the PDSs for a large sample of bursts. It indicates that different GRBs are random realizations of the same stochastic process. The power-law PDS provides a new sensitive tool for studies of gamma-ray bursts. In particular, we calculate the PDSs of bright bursts in separate LAD energy channels. The average PDS flattens in the hardest channel ($h\nu > 300$ keV) and steepens in the softest channel ($h\nu < 50$ keV). The average PDS of bolometric light curves has a slope $\alpha \approx -5/3$ and a sharp high frequency break at ~ 1 Hz.

INTRODUCTION

Contrary to the complicated diverse behavior in the time domain, long GRBs show a simple behavior in the Fourier domain (Beloborodov, Stern, & Svensson 1998). Their PDS is a power-law of index $\alpha \approx -5/3$ (with a high frequency break at ~ 1 Hz) plus standard (exponentially distributed) statistical fluctuations superimposed onto the power law. The $-5/3$ slope and the 1 Hz break characterize the process randomly generating the diverse light curves of GRBs. Intriguingly, the PDS slope coincides with the Kolmogorov law.

Here, we illustrate the power law seen in the longest bursts, present the average PDS for an extended sample of GRBs, and compare the PDSs in separate energy channels. We quantify the difference of the temporal structure between the channels in terms of the PDS slope and compare the results with previous studies of the autocorrelation function (ACF). An extended description of this work is given in Beloborodov (1999) and Beloborodov, Stern, & Svensson (2000).

In our analysis, we use GRB light curves with 64 ms resolution obtained by BATSE in the four LAD energy channels, I–IV: (I) $20-50$ keV, (II) $50-100$ keV, (III) $100-300$ keV, and (IV) $h\nu > 300$ keV. The background is subtracted using linear fits to the 1024 ms data. Our sample consists of 527 GRBs with $T_{90} > 20$ s and the peak flux in channels II+III, $C_{\rm peak} > 100$ counts per 64 ms time bin.

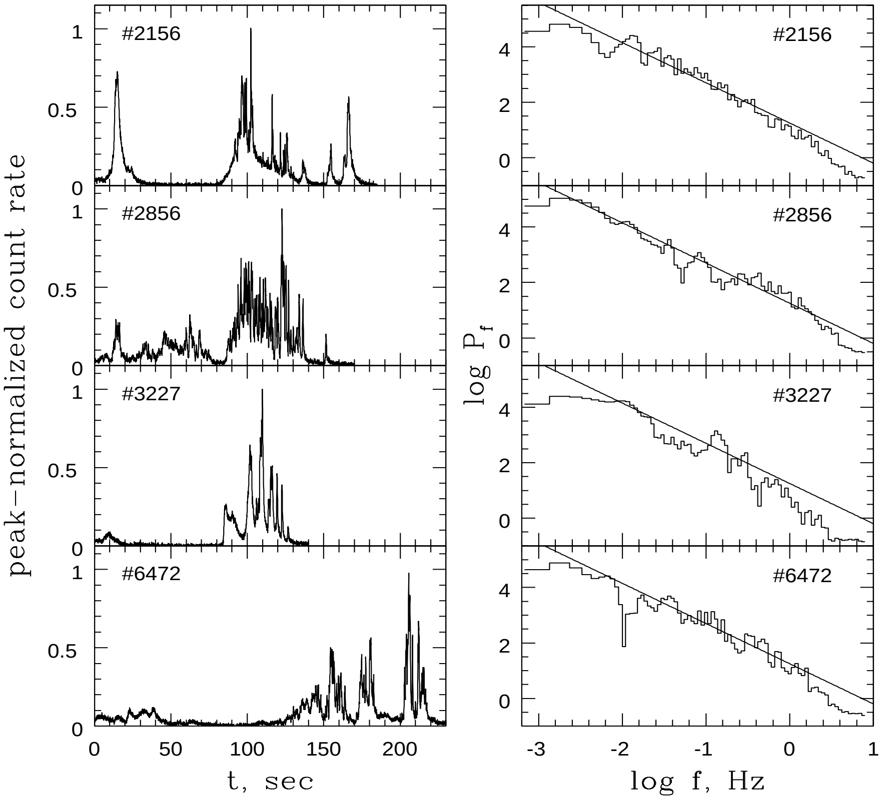

FIGURE 1. The light curves (in channels II+III) and their PDSs for the four brightest bursts in the sample with $T_{90} > 100$ s. The light curves are peak-normalized and, correspondingly, the PDSs are normalized by $C^2_{\rm peak}$. We smoothed the PDSs on the scale $\Delta \log f = 0.04$ before the plotting. The straight lines show the fit to the average of the 4 PDSs, $\log P_f = 1.25 - 1.45 \log f$.

INDIVIDUAL POWER DENSITY SPECTRA

The four brightest bursts with $T_{90} > 100$ s in our sample have trigger numbers # 2156, 2856, 3227, and 6472. To simplify the comparison of different bursts, we use peak-normalized light curves, $C(t)$. Their Fourier transform, C_f, is therefore normalized by $C_{\rm peak}$, and the PDS, $P_f = C_f C^*_f$, is normalized by $C^2_{\rm peak}$. The light curves and their PDSs are shown in Figure 1. The light curves are very different while the PDSs are similar. They can be described as a single power law, $\log P_f = A + \alpha \log f$ ($A \approx 1$ and $\alpha \approx -1.5$) with super-imposed fluctuations $\Delta P_f / P_f \sim 1$. In spite of the large ΔP_f, the power-law behavior can be seen in each burst due to the power-law extending over more than two decades in frequency.

The PDS analysis was previously performed for a number of individual bursts. Belli (1992) analyzed GRBs detected by the Konus experiment and Giblin, Kouveliotou, & van Paradijs (1998) studied individual BATSE bursts. The power-law PDS can be observed in their longest complex bursts as well.

THE AVERAGE PDS OF GRBS

In most of the GRB models (e.g., in the internal shock model), different bursts are produced by one physical mechanism of a stochastic nature, i.e., an individual burst is a random realization of the same standard process. With such an approach, individual GRBs are like pieces of a "puzzle", and the features of the standard engine can be probed with statistical methods applied to a large ensemble of GRBs.

The simplest statistical characteristic of the PDSs is the average PDS. The average PDS, $\bar{P}_f$, for the 527 peak-normalized light curves in LAD channels (II+III) is shown in Figure 2. For comparison, we also plot the average PDS for light curves normalized by $\sqrt{\Phi}$, where Φ is the burst fluence. The average PDS then has a different amplitude. Nevertheless, $\bar{P}_f$ again follows a power-law with approximately the same slope. This provides evidence that the self-similar behavior with $\alpha \approx -5/3$ is an intrinsic property of GRBs, rather than an artifact of the averaging procedure. This interpretation is also supported by the fact that we observe the same power-law behavior for the longest individual bursts (see Fig. 1). Note also that the distribution of P_f around $\bar{P}_f$ is self-similar with respect to shifts in f (see Beloborodov, Stern, & Svensson 1998). The self-similar behavior breaks at ~ 1 Hz.

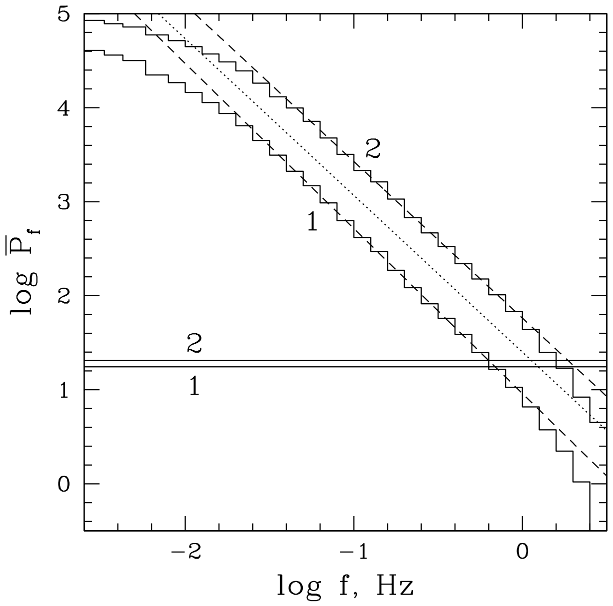

FIGURE 2. The average PDS (in LAD channels II+III) for the full sample of 527 GRBs. The histograms marked as 1 and 2 correspond to the peak-normalization and the $\sqrt{\Phi}$-normalization, respectively. The horizontal lines show the corresponding normalized Poisson levels averaged over the sample. *Dashed lines* are the power-law fits in the range $-1.4 < \log f < -0.1$: $\log \bar{P}_f = 0.96 - 1.75 \log f$ in the peak-normalized case and $\log \bar{P}_f = 1.76 - 1.67 \log f$ in the $\sqrt{\Phi}$-normalized case. The *dotted line* shows the $-5/3$ slope.

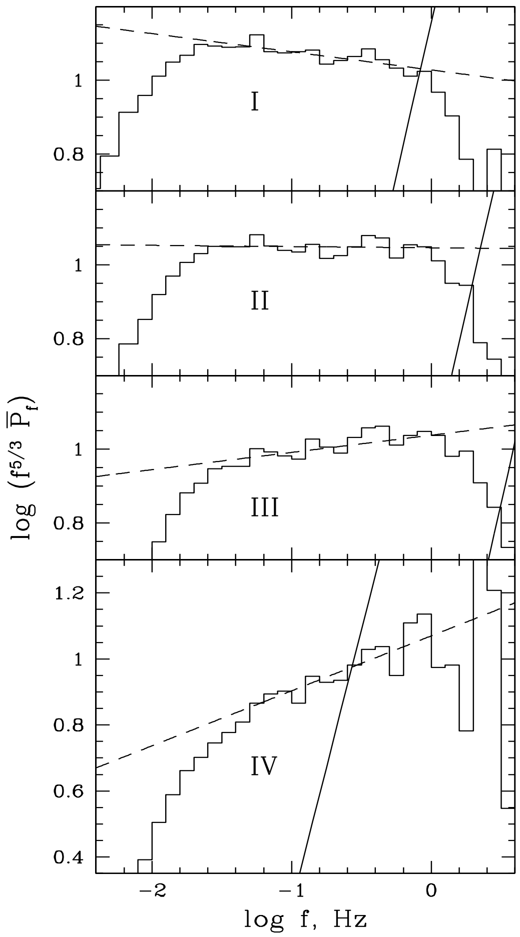

FIGURE 3. The average PDS for the sample of 152 GRBs in separate energy channels, I, II, III, and IV. *Dashed lines* show the power-law fits (see Table 1). *Solid lines* show the Poisson level.

PDS AND ACF IN SEPARATE LAD CHANNELS

The average PDSs for the brightest 152 bursts in LAD channels I–IV are shown in Figure 3. The differences in the slopes are clearly seen. We fitted the PDSs by power laws, $\log \bar{P}_f = A + \alpha \log f$, in the range $-1.6 < \log f < 0$. Channel IV is fitted in the range $-1.3 < \log f < -0.1$. A and α of the fits are listed in Table 1.

TABLE 1. Fitting parameters for the average PDS and ACF

Channel	PDS slope, α	PDS amplitude, A	ACF index, β	ACF width, τ_0
I	−1.72	1.03	0.73	14.0
II	−1.67	1.05	0.67	10.7
III	−1.60	1.06	0.63	7.3
IV	−1.50	1.07	0.6	5.1

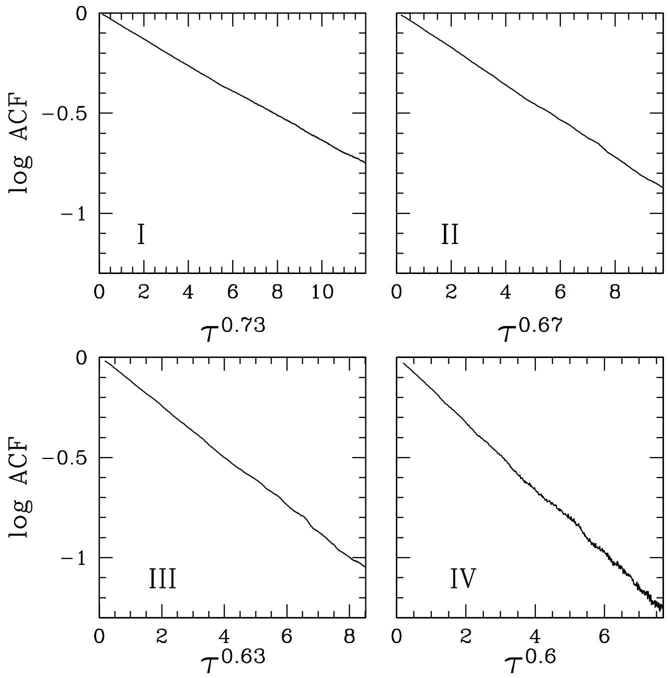

FIGURE 4. The average ACFs in channels I-IV are plotted against τ^β which should give a straight line for a stretched exponential.

The autocorrelation function (ACF) contains the same information as the PDS since one is the Fourier transform of the other (the Wiener-Khinchin theorem). The average ACF, $\bar{A}(\tau)$, for our sample of 152 bright GRBs is shown in Figure 4. In each channel, the ACF is perfectly fitted by a stretched exponential: $\bar{A}(\tau) = \exp(-[\tau/\tau_0]^\beta)$. The parameters τ_0 and β are listed in Table 2. Note the approximate relation between the ACF index, β, and the PDS slope, α, $\beta \approx -(1+\alpha)$. τ_0 measures the ACF width. The ACF gets narrow at high energies, in agreement with previous studies (Fenimore et al. 1995).

REFERENCES

1. Belli, B. M., *ApJ*, **393**, 266 (1992).
2. Beloborodov, A. M., in ASP Conf. Ser., *Gamma-Ray Bursts: The First Three Minutes*, eds. J. Poutanen & R. Svensson (San Francisco: ASP), **190**, 47 (1999)
3. Beloborodov, A. M., Stern, B. E., and Svensson, R., *ApJ*, **508**, L25 (1998).
4. Beloborodov, A. M., Stern, B. E., and Svensson, R., *ApJ*, in press (2000), astro-ph/0001401
5. Fenimore, E. E., et al., *ApJ*, **448**, L101 (1995).
6. Giblin, T. W., Kouveliotou, C., and van Paradijs, J., in AIP Conf. Proc. **428**, *Gamma-Ray Bursts*, eds. C. A. Meegan, R. D. Preece, & T. M. Koshut, (New York: AIP), 241 (1998).